Proc. Natl. Acad. Sci. USA
Vol. 91, pp. 5207–5211, May 1994
Neurobiology

Calcium transients in dendrites of neocortical neurons evoked by single subthreshold excitatory postsynaptic potentials via low-voltage-activated calcium channels

(dendritic Ca^{2+})

HENRY MARKRAM AND BERT SAKMANN

Max-Planck-Institut für Medizinische Forschung, Abteilung Zellphysiologie, Jahnstrasse 29, D-69120 Heidelberg, Germany

Contributed by Bert Sakmann, February 7, 1994

ABSTRACT **Simultaneous recordings of membrane voltage and concentration of intracellular Ca^{2+} ($[Ca^{2+}]_i$) were made in apical dendrites of layer 5 pyramidal cells of rat neocortex after filling dendrites with the fluorescent Ca^{2+} indicator Calcium Green-1. Subthreshold excitatory postsynaptic potentials (EPSPs), mediated by the activation of glutamate receptor channels, caused a brief increase in dendritic $[Ca^{2+}]_i$. This rise in dendritic $[Ca^{2+}]_i$ was mediated by the opening of low-voltage-activated Ca^{2+} channels in the dendritic membrane. The results provide direct evidence that dendrites do not function as passive cables even at low-frequency synaptic activity; rather, a single subthreshold EPSP changes the dendritic membrane conductance by opening Ca^{2+} channels and generating a $[Ca^{2+}]_i$ transient that may propagate towards the soma. The activation of these Ca^{2+} channels at a low-voltage threshold is likely to influence the way in which dendritic EPSPs contribute to the electrical activity of the neuron.**

Glutamate mediates excitatory synaptic input to pyramidal neurons in mammalian neocortex by activating both the L-α-amino-3-hydroxy-5-methyl-4-isoxazoleproprionate (AMPA) receptor (AMPA-R) and *N*-methyl-D-aspartate (NMDA) receptor (NMDA-R) channels (1, 2). It has recently been shown that neocortical pyramidal dendrites are not passive but can support action potentials (APs) (3–6). Surprisingly, these APs arise in the initial axon segment and then back-propagate into the dendrites (6). This back-propagation suggests that the AP serves as a retrograde message of the status of AP firing rather than a mechanism of amplifying the effect of excitatory postsynaptic potentials (EPSPs) on the soma. The back-propagating AP activates voltage-activated Ca^{2+} channels (VACCs) of several subtypes and generates a dendritic Ca^{2+} concentration transient ($[Ca^{2+}]_i$) (7). The AP-dependent dendritic transient $[Ca^{2+}]_i$ is likely to mediate the signal that the AP conveys to dendrites. In hippocampal pyramidal cells, tetanic synaptic stimulation has been shown to cause $[Ca^{2+}]_i$ increases in the dendrite attributable to the activation of VACCs (8). The question arises whether single EPSPs, generated by AMPA-R and NMDA-R channel activation, are sufficient to trigger opening of VACCs and thereby cause a transient increase in dendritic $[Ca^{2+}]_i$ before AP threshold is reached.

We tested this possibility by determining the amplitude and time course of the increase in $[Ca^{2+}]_i$ in dendrites during a subthreshold dendritic EPSP, recorded with a dendritic pipette and loaded with the Ca^{2+}-sensitive indicator Calcium Green-1. We found that the dendritic depolarization during a single EPSP is sufficient to generate a transient increase in dendritic $[Ca^{2+}]_i$ via activation of VACCs.

The publication costs of this article were defrayed in part by page charge payment. This article must therefore be hereby marked "*advertisement*" in accordance with 18 U.S.C. §1734 solely to indicate this fact.

MATERIALS AND METHODS

Electrophysiology. Methods similar to those described previously were used (9). Briefly, neocortical slices from Wistar rats were incubated and then perfused (20–22°C) in a standard bicarbonate Ringer's solution containing 4 mM $CaCl_2$ and 4 mM $MgCl_2$ to reduce synaptic noise. Layer 5 pyramidal cells were identified using IR differential interference contrast video-microscopy on an upright microscope (9). The microscope stage was rotated so that the apical dendrite was parallel to the scanning direction of the fast mirror of a confocal laser scanning microscope (CLSM; Phoibos 1000, MD). Somatic whole-cell and dendritic whole-cell recordings were made with an EPC-7 and an EPC-9 amplifier (List Electronics, Darmstadt, Germany), respectively. Dendritic patches were typically 70–110 μm from the soma. For current-clamp recordings, bridge balancing was performed by using the series resistance compensation of the EPC-9. For voltage-clamp recordings from dendrites, pipette capacitance, whole-cell capacitance, and series resistances (40–50%) were compensated. Neurons were recorded with pipettes containing 100 mM potassium gluconate, 20 mM KCl, 4 mM Mg-ATP, 10 mM phosphocreatine, 50 units of creatine phosphokinase per ml, 0.3 mM GTP, 10 mM Hepes (pH 7.3, 310 milliosmolar). Calcium Green-1 (100 μM; Molecular Probes, 488-nm excitation, emission 515–560 nm, 530-nm peak, K_d = 239 nm) was loaded into cells, and fluorescence (F) was imaged with the CLSM controlled by an IRIS computer (model 4D35, Silicon Graphics, Mountain View, CA).

Synaptic Stimulation. To isolate NMDA-R-mediated EPSPs, slices were superperfused with normal Ringer's solution containing 4 mM $CaCl_2$, 4 mM $MgCl_2$, 5 μM picrotoxin (Sigma) or 5 μM bicuculline [Research Biochemicals Incorporated (RBI)], 5 μM phaclophen (Calbiochem) or 10 μM saclophen (Tocris Neuramin, Bristol, U.K.), and 20 μM 6-cyano-7-nitroquinoxaline-2,3-dione (CNQX; Tocris). Phaclophen was used in all cases except in the voltage-clamp experiments, where scalophen was used (see Fig. 5). To block the slow EPSP, 50 μM D-(−)-2-amino-5-phosphonopentanoic acid (D-AP5; Tocris) was added to the extracellular bath solution. A monopolar tungsten electrode of 2- to 3-ohm resistance was placed in layer 2, and stimulus pulses of 15–20 V for 10–50 μs were applied. To block APs, lidocaine *N*-ethylbromide quaternary salt (10 mM, QX-314; RBI) was placed in the pipette.

Ca^{2+} Fluorescence Imaging. Confocality increased sampling errors that arose from the difficulty to focus equally

Abbreviations: EPSP, excitatory postsynaptic potential; EPSC, excitatory postsynaptic current; AMPA-R, L-α-amino-3-hydroxy-5-methyl-4-isoxazolepropionate receptor; NMDA-R, *N*-methyl-D-aspartate receptor; AP, action potential; F, fluorescence; V_m, membrane potential; $[Ca^{2+}]_i$, concentration of intracellular Ca^{2+} transients; CLSM, confocal laser scanning microscope; D-AP5, D-(−)-2-amino-5-phosphonopentanoic acid.

along the length of the dendrite; hence, experiments were performed in the nonconfocal mode. Laser power of all lines was set to 20 mW, and the photomultiplier voltage was adjusted to accommodate the dynamic range of ΔF. The dendrite was scanned in the "line-scan mode"—namely, the laser beam was directed as a single line (1.3-μm width of dendrite was sampled) along the length of the dendrite (20 ms per line). Typically 128 consecutive line-scans were executed. Stimuli were applied after 500 ms of basal fluorescence (F_{basal}) recording. Bleaching during the 128 line-scans that were ordinarily used was usually undetectable. In some cases, however, a control scan series without stimulation, was used to correct for bleaching. The apical dendrite was scanned up to 160 μm from the soma. Fluorescence data are presented as either ΔF ($F - F_{basal}$) or % ΔF $\{[(F - F_{basal})/F_{basal}] \times 100\}$. F_{basal} was the average fluorescence level 500 ms before a stimulus. The fluorescence responses were recorded in photomultiplier tube (PMT) units (0–255). In some cases, to obtain below a PMT unit resolution, the dendritic region analyzed was subdivided into sections, and sections were averaged individually. The average fluorescence of three points from and including the peak were used to quantify control ΔF responses. The same time points were averaged in the response during a given drug application.

RESULTS

Simultaneous Monitoring of Subthreshold EPSPs and Ca^{2+} Fluorescence. We used IR differential interference contrast imaging of neurons in brain slices (9) to select pyramidal neurons according to their shape—in particular those with apical dendrites that lay in the horizontal plane of focus. A patch-pipette containing Calcium Green-1 was sealed to the dendrite of an identified neuron, and Ca^{2+}-dependent changes in fluorescence were monitored with a temporal resolution of 20 ms via CLSM imaging (7). Fig. 1 *Upper Left* shows a pyramidal cell in the cortical brain slice filled with Calcium Green-1. Fluorescence changes in the apical dendrite were monitored repeatedly by a line-scan along the dendrite between the two arrows. In Fig. 1 *Upper Right*, the time-dependent changes at different parts of the dendrite from the soma towards the tufts are illustrated as they occur before and after an EPSP. The EPSP, as shown on the same time scale in the trace in Fig. 1 *Lower* was generated by an electric stimulus applied to afferents in cortical layer 2. In Fig. 1 *Lower* the time course of the stimulus-evoked change in fluorescence (ΔF) and the EPSP (V_m) recorded by the dendritic pipette are compared. The time courses match well at the peak, although the $[Ca^{2+}]_i$ transient decays more slowly. Subthreshold EPSPs evoked a detectable $[Ca^{2+}]_i$ transient in 28 of 33 dendrites. The question then arises whether the $[Ca^{2+}]_i$ increase is mediated by inflow of Ca^{2+} through Ca^{2+}-permeable NMDA-R or AMPA-R channels or by activation of the metabotropic glutamate receptor by inflow through VACCs in the dendritic membrane.

Voltage Dependence of EPSP-Triggered Increase in Dendritic $[Ca^{2+}]_i$. To determine the mechanism of the EPSP-triggered $[Ca^{2+}]_i$ transient, we first examined whether the transient was voltage-dependent and whether directly depolarizing the dendritic membrane could evoke Ca^{2+} entry in a voltage-dependent manner. Fig. 2*A* shows simultaneous records of ΔF (upper traces) and dendritic V_m (lower traces) following stimulation with different stimulus strengths of excitatory afferents. The changes in V_m and ΔF suggest a characteristic voltage-dependent behavior. When, during the EPSP, the dendritic membrane was depolarized from −60 mV to below −40 mV, a fluorescence change was barely detectable. However, at more positive potentials, ΔF increased abruptly. Since at least a 2% ΔF is required to cause a signal clearly above noise, the EPSP-evoked Ca^{2+} entry

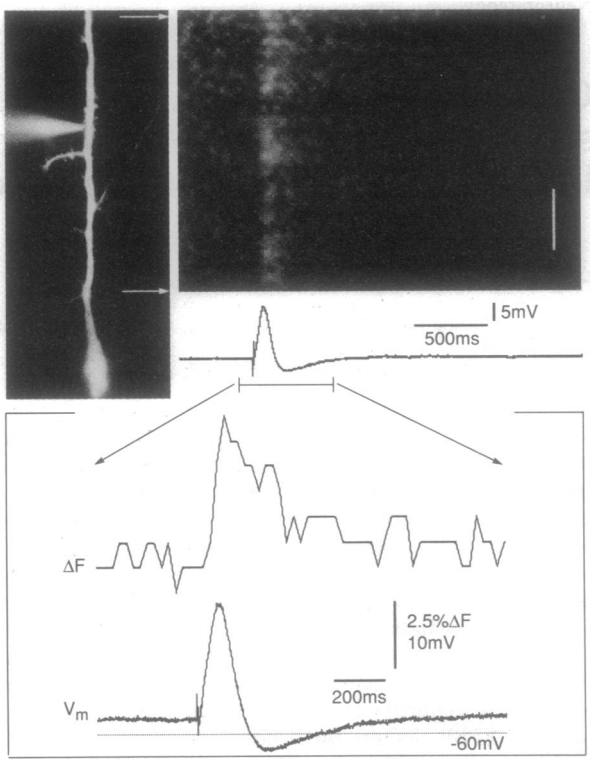

FIG. 1. Dendritic $[Ca^{2+}]_i$ transients and subthreshold dendritic EPSP evoked by synaptic stimulation. Fluorescence changes (ΔF) in the apical dendrite of a pyramidal cell evoked by a stimulus-evoked NMDA-R-mediated EPSP. (*Upper Left*) Pyramidal cell loaded with Calcium Green-1 from a patch-pipette sealed to the dendrite. The length of the line-scan is marked by arrows. (*Upper Right*) Record of 128 consecutive line scans. The image represents %ΔF (gray-scale) with time (x axis) and corresponding dendrite position (y axis). Trace below shows the dendritic V_m before, during, and after electric stimulation of afferents in cortical layer 2. (*Lower*) Shows average dendritic ΔF (upper trace) of the entire dendritic region scanned and dendritic V_m (lower trace) at higher resolution. (Bar = 20 μm and applies to *Upper Left* and *Upper Right*.)

may begin at somewhat lower voltages. The ΔF detected when the ramp V_m was changed to range from −60 mV to −35 mV compares well with that evoked by the EPSPs. By averaging several experiments, it was found that the Ca^{2+} entry was detectable from dendritic membrane potentials of −50 mV and increased in size approximately linearly to below AP threshold (Fig. 2*B*). Action potential threshold was reached at −35 ± 3 mV (n = 34; mean ± SD). The voltage dependence of ΔF induced by EPSPs suggests that the fluorescence changes are associated with the activation of VACCs and/or by Ca^{2+} entry through NMDA-R channels, which, in the presence of extracellular Mg^{2+}, may produce a comparable ΔF–V_m relationship. Before dissecting the contribution of NMDA-R channels and VACCs, we first blocked the NMDA receptor and measured the $[Ca^{2+}]_i$ transient evoked by an EPSP that was generated by AMPA-R activation alone.

Single Subthreshold AMPA-R-Mediated EPSPs Evoke an Increase in $[Ca^{2+}]_i$. Fig. 3 shows a sub- and suprathreshold EPSP mediated by NMDA-R channels evoking a $[Ca^{2+}]_i$ transient in the dendrite. The amplitude of the $[Ca^{2+}]_i$ transient evoked by the subthreshold EPSP (Fig. 3*A Left*) was approximately one-third of that evoked by the suprathreshold EPSP and AP (n = 26) (Fig. 3*A Right*). The largest subthreshold $[Ca^{2+}]_i$ transient evoked by depolarizing current pulses was also about one-third of that triggered by a back-propagating AP (n = 34). The $[Ca^{2+}]_i$ transient evoked by an AMPA-R-mediated EPSP to −40 mV was comparable to that

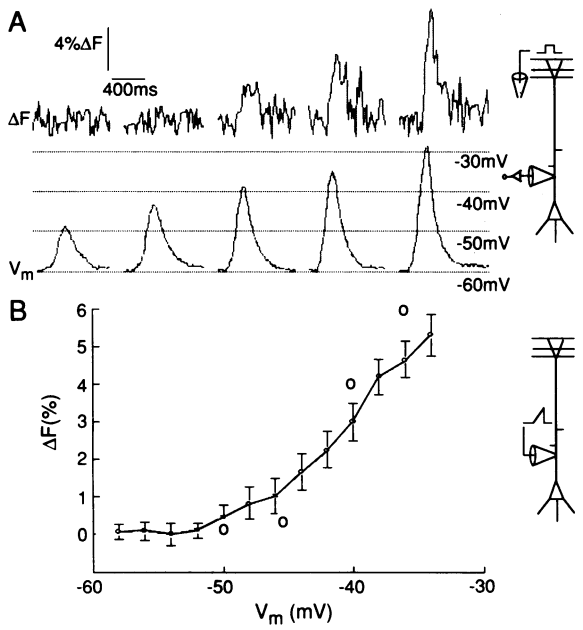

FIG. 2. Voltage dependence of dendritic $[Ca^{2+}]_i$ transients evoked by EPSP and depolarization via current injection. (*A*) Simultaneous recording of ΔF and V_m in apical dendrite, evoked by NMDA-R-mediated EPSPs. Dendrite was loaded with QX-314, and afferents in cortical layer 2 were stimulated electrically with progressively stronger stimuli. When V_m reached −40 mV, a ΔF response was detectable. (*B*) Mean ΔF during change of ramp V_m (mean ± SD, $n = 11$). o, ΔF values of the experiment shown in *A*. The average ΔF within 30–40 μm on either side of the patch-pipette are represented. Logos on the right represent the neuron and positions of the recording and stimulating pipettes.

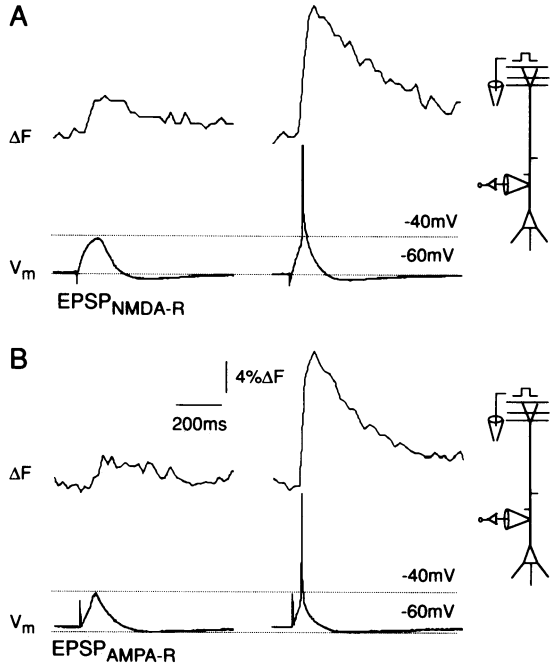

FIG. 3. Dendritic $[Ca^{2+}]_i$ transients triggered by NMDA-R- and AMPA-R-mediated EPSPs. (*A*) Transient in ΔF triggered by dendritic NMDA-R-mediated EPSP (*Left*) is roughly one-third of that triggered by a single dendritic AP (*Right*). (*B*) Transient in ΔF triggered by dendritic AMPA-R-mediated EPSP (*Left*) and suprathreshold EPSP and AP (*Right*). The amplitudes of ΔF and the approximate ratio of ΔF caused by a single AP are similar in both experiments. The average ΔF values within 50 μm on either side of the patch-pipette are represented. For logo, see Fig. 2 legend.

of the NMDA-R-mediated EPSPs (Fig. 3*B*; $n = 5$). Since possible Ca^{2+} entry through AMPA-R channels is expected to be less than that potentially caused by NMDA-R channels (10, 11), it appears likely that most of the Ca^{2+} entry triggered by the AMPA-R-mediated EPSP in the dendritic trunk, is secondary to the depolarization of the dendritic membrane.

Depolarizing Dendrites Mimics the EPSP-Evoked Ca^{2+} Fluorescence Signal. Further evidence for the dependence of the EPSP-evoked $[Ca^{2+}]_i$ transient on the activation of VACCs is provided by experiments where the dendritic $[Ca^{2+}]_i$ increase was measured for evoked EPSPs and compared with membrane potential transients evoked by current injection through the recording pipette (simulated EPSPs). They resemble closely synaptic EPSPs in terms of their amplitude and time course. Fig. 4 compares the changes in V_m and ΔF for the two conditions. Both synaptic and simulated EPSPs generated $[Ca^{2+}]_i$ transients of comparable amplitude and time course. While the synaptic EPSP and the associated $[Ca^{2+}]_i$ transient were reversibly abolished by the NMDA receptor blocker D-AP5, the $[Ca^{2+}]_i$ transient evoked by the simulated EPSP remained unchanged. This experiment suggests (*i*) that the contribution of the metabotropic glutamate receptor to the detected Ca^{2+} entry was negligible, (*ii*) that the Ca^{2+} entry triggered by direct V_m depolarization was not due to the opening of NMDA-R channels that were associated with ambient glutamate (12), and (*iii*) that dendritic depolarization to subthreshold potentials (in a manner similar to that of the EPSP) can indeed trigger Ca^{2+} entry through VACCs.

Additional evidence that the detected $[Ca^{2+}]_i$ transient during a synaptic EPSP is primarily caused by Ca^{2+} entry through VACCs is illustrated in Fig. 5. Under current-clamp conditions, the EPSP generates a clear $[Ca^{2+}]_i$ transient (Fig. 5*A*). On the other hand, in locally voltage-clamped dendrites, neither the excitatory postsynaptic current (EPSC) at −60 mV nor that at −40 mV (Fig. 5 *B* and *C*), which corresponds to the peak depolarization of the EPSP, generated a $[Ca^{2+}]_i$ transient ($n = 7$). During more restricted afferent stimulation, better achieved with low-intensity electrical stimuli and more than 200 μm from the soma, the amplitude of NMDA-R-mediated EPSC at −60 mV is less than half that at −40 mV and virtually absent at −80 mV ($n = 3$; data not shown), suggesting that part of the current in Fig. 5 *B* and *C* reflects current through unclamped, more distal synapses.

Effect of Ca^{2+} Channel Antagonists on Synaptically and Nonsynaptically-Triggered Ca^{2+} Entry. To confirm that the ΔF transients evoked by synaptic and simulated EPSPs were indeed mediated by Ca^{2+} entry through VACCs, we examined the effect of Ca^{2+} channel blockers on the measured ΔF. Traces in Fig. 6*A Upper* and *Middle* show that Cd^{2+}, used at a concentration that would block most Ca^{2+} channels, blocked the ΔF caused by a simulated EPSP. In nine experiments, Cd^{2+} reduced the depolarization-evoked $[Ca^{2+}]_i$ transient to 7 ± 1.5% of control (mean ± SEM, $P < 0.05$; paired *t* test), confirming that the ΔF transients were due to changes in $[Ca^{2+}]_i$. In Fig. 6*A Bottom*, the middle trace shows the effect of Cd^{2+} on AP frequency accommodation. Cd^{2+} blocked AP frequency accommodation, which arises partly from the activation of Ca^{2+}-activated K^+ channels (13), providing further evidence to suggest that Ca^{2+} entry was blocked. Since Cd^{2+} also abolished the synaptic EPSP completely, we examined the effect of Ni^{2+}, a Ca^{2+} channel blocker with a higher affinity for low VACCs (14). The EPSP and the $[Ca^{2+}]_i$ transient were differentially sensitive to Ni^{2+} as illustrated in Fig. 6*B*. Ni^{2+} (100 μM) reduced the peak of the EPSP from −35 to −40 mV and nearly abolished the $[Ca^{2+}]_i$ transient ($n = 5$). We further examined the effect of Ni^{2+} on the $[Ca^{2+}]_i$ transient caused by dendritic current injection. Ni^{2+} at a concentration of 10 μM reduced the evoked $[Ca^{2+}]_i$ transient to 68 ± 4% of control ($n = 7$; $P <$

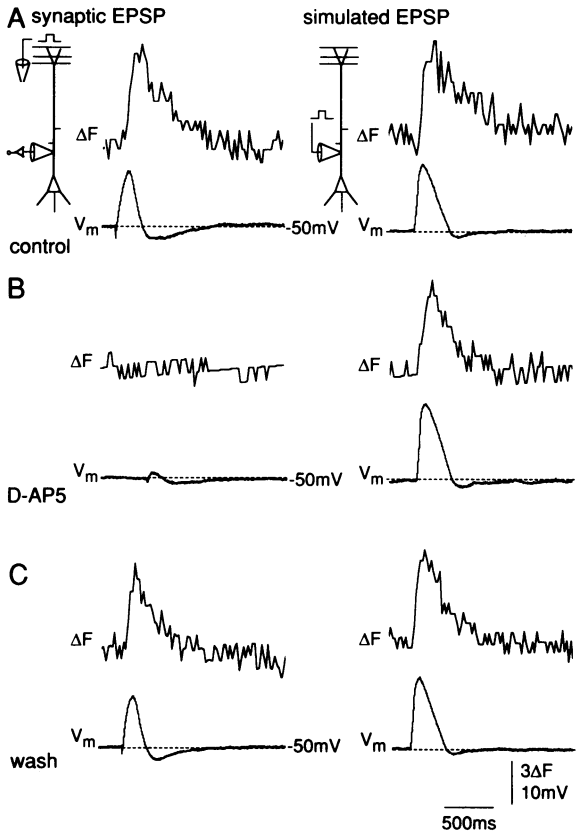

FIG. 4. Comparison of dendritic $[Ca^{2+}]_i$ transients during EPSPs and depolarization via current injection. (*A*) Changes in ΔF during EPSPs (*Left*) and depolarization generated by current injection (*Right*). Depolarization ("simulated" EPSPs) were generated by current injection via dendritic pipette with a linear current ramp that peaked within 20 ms and decayed within 200 ms. The resultant ΔF and V_m changes are comparable for synaptic and "simulated" EPSPs. (*B*) In the presence of D-AP5, a blocker of NMDA-R channels, ΔF and V_m changes evoked by synaptic stimulation are abolished while those generated by current injection were unaffected. (*C*) Control after washout of D-AP5. The ΔF values within 20 μm on either side of the patch-pipette are represented.

0.05; paired *t* test; data not shown) and to 17 ± 4% of control at a concentration of 100 μM ($n = 5$; $P < 0.05$; paired *t* test; data not shown), suggesting that the effect of Ni^{2+} on the EPSP-evoked $[Ca^{2+}]_i$ transient may also have been due to the

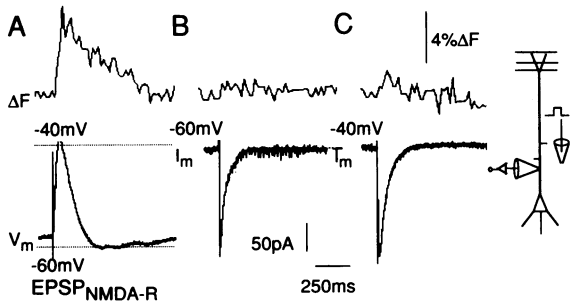

FIG. 5. Activation of NMDA-R channels does not contribute significantly to EPSP-evoked dendritic $[Ca^{2+}]_i$ transient. (*A*) ΔF transient (upper trace) evoked by the NMDA-R-mediated EPSP (lower trace). (*B* and *C*) NMDA-R-mediated EPSCs failed to evoke a significant ΔF transient at −60 mV and insignificant ΔF transient at −40 mV. Actual basal *F* is increased at −40 mV (not shown). Afferents were stimulated electrically in the region of the recording to evoke EPSP or EPSC by local voltage clamp. The ΔF with 20 μm on either side of the patch-pipette was measured. For logo, see Fig. 2 legend.

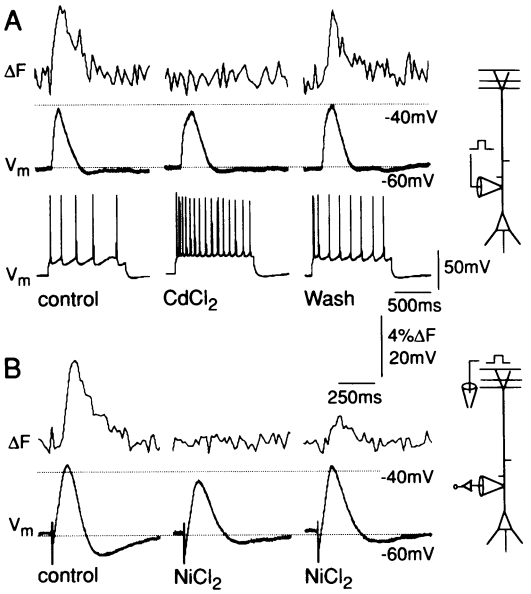

FIG. 6. Block of voltage-activated Ca^{2+} channels reduces EPSP-evoked $[Ca^{2+}]_i$ transients. (*A*) Effect of Cd^{2+} (200 μM) on ΔF transient (top trace) evoked by depolarization through current injection (middle trace). The left set of traces represents controls, center set was recorded during Cd^{2+} superfusion, and the right set was recorded after wash-out of Cd^{2+}. Bottom traces in each set show the block of frequency accommodation of dendritic APs by Cd^{2+}. (*B*) Ni^{2+} (100 μM) blocked most of the dendritic $[Ca^{2+}]_i$ transient and reduced the peak of the dendritic EPSP (left and center traces). The right traces show the $[Ca^{2+}]_i$ transient when the stimulus intensity was increased to match that of the control. ΔF was measured within 30 μm on either side of the patch-pipette.

blockade of VACCs on the dendrite. However, the EPSP- and depolarizing current-evoked $[Ca^{2+}]_i$ transients were unaffected by 50 μM amiloride ($n = 11$; data not shown), a blocker of the low-threshold T-type Ca^{2+} channel (15).

DISCUSSION

The experiments indicate that a single subthreshold dendritic EPSP, mediated by the opening of glutamate receptor channels in apical dendrites of cortical pyramidal cells, generates a transient increase in dendritic $[Ca^{2+}]_i$. The EPSP-evoked $[Ca^{2+}]_i$ transient is comparable to the dendritic EPSP in the time course to peak but decays more slowly. Depolarizations caused by current injection produced changes in $[Ca^{2+}]_i$ that were comparable to those produced by dendritic EPSPs and that were insensitive to NMDA-R blockade but sensitive to the blockade of VACCs. Similarly, the NMDA-R-mediated EPSPs produced a $[Ca^{2+}]_i$ transient that was independent of NMDA-R current but was dependent on NMDA-R-mediated depolarization and on the integrity of VACCs. AMPA-R-mediated EPSPs also evoked a $[Ca^{2+}]_i$ transient. These results strongly suggest that the EPSP-evoked $[Ca^{2+}]_i$ transient was generated via the opening of VACCs in the dendritic membrane (see also ref. 8). Because we can not be certain that synapses within the scanned regions were activated by afferent stimulation and because of a potential difficulty in detecting highly localized Ca^{2+} entry, the results do not exclude Ca^{2+} inflow via NMDA-R channels (see refs. 16–19).

The size of the largest $[Ca^{2+}]_i$ transient generated by a single subthreshold EPSP is substantial, since it may amount to about one-third of the $[Ca^{2+}]_i$ transient generated by a back-propagating dendritic AP (Fig. 3 and ref. 7). The $[Ca^{2+}]_i$ transient may be sufficient to cause a small but detectable activation of Ca^{2+}-dependent K^+ channels as suggested by

the shape of the simulated EPSPs (Fig. 4) and the effect of Cd^{2+} (Fig. 6*A*) and Ni^{2+} (Fig. 6*B*). The "undershoot" may also be due to the activation of an I_H current (slow inward rectifier) (20) and, in the case of the synaptic EPSPs, may also represent a component generated by incompletely blocked γ-aminobutyric acid type B receptor channels (Fig. 6*B*).

Under physiological conditions, an EPSP-evoked $[Ca^{2+}]_i$ transient would occur after the summation of a number of unitary EPSPs and thus may represent the integrated result of dendritic activity at a given moment in time and a given position of the dendrite. The dendritic parts involved in this transient would depend on the site of origin of the EPSPs along the dendritic tree, spatial and temporal summation, and the attenuation of EPSPs as they spread towards the soma or towards more peripheral parts of the dendritic tree. Therefore, this $[Ca^{2+}]_i$ transient is likely to be restricted to certain regions of the dendritic tree.

A number of possible physiological functions for the EPSP-evoked $[Ca^{2+}]_i$ transient exists. First, this $[Ca^{2+}]_i$ transient may act to provide a "dendritic record" of a progressively more integrated version of the synaptic input and thus may serve to signal the status of the integration to the dendrites. Since intracellular Ca^{2+} may activate biochemical pathways (21, 22), this signal may be long lasting. Second, the $[Ca^{2+}]_i$ transient may not be restricted only to the dendritic shaft but may spread into dendritic spines, providing a "coupling" between synapses. Such coupling would then depend on the ability of the dendritic Ca^{2+} to reach the spine head (see refs. 23, 24). Finally, since Ca^{2+} channels are involved, the integration of EPSPs may be directly influenced by being amplified as the V_m depolarizes above -50 mV (see ref. 25).

We thank Drs. N. Spruston, M. Segal, W. Betz, L. P. Wollmuth, M. J. Gutnick, and E. Neher for helpful comments on the manuscript. The work was supported by the Minerva Foundation.

1. Tsumoto, T., Hagihara, K., Sato, H. & Hata, Y. (1987) *Nature (London)* **327**, 513–514.
2. Miller, K. D., Chapman, B. & Stryker, M. P. (1989) *Proc. Natl. Acad. Sci. USA* **86**, 5183–5187.
3. Huguenard, J. R., Hamill, O. P. & Prince, D. A. (1989) *Proc. Natl. Acad. Sci. USA* **86**, 2473–2477.
4. Amitai, Y., Friedman, A., Connors, B. W. & Gutnick, M. J. (1993) *Cereb. Cortex* **3**, 26–38.
5. Regehr, W., Kehoe, J., Ascher, P. & Armstrong, C. (1993) *Neuron* **11**, 145–151.
6. Stuart, G. J. & Sakmann, B. (1994) *Nature (London)* **369**, 69–72.
7. Markram, H., Sakmann, B. & Helm, P. J. (1994) *J. Physiol. (London)*, in press.
8. Miyakawa, H., Ross, W. N., Jaffe, D., Callaway, J. C., Lasser-Ross, N., Lisman, J. E. & Johnston, D. (1992) *Neuron* **9**, 1163–1173.
9. Stuart, G. J., Dodt, H.-U. & Sakmann, B. (1993) *Pflügers Arch.* **423**, 511–518.
10. Iino, M., Ozawa, S. & Tsuzuki, K. (1990) *J. Physiol. (London)* **424**, 151–165.
11. Schneggenburger, R., Zhou, Z., Konnerth, A. & Neher, E. (1993) *Neuron* **11**, 133–143.
12. Sah, P., Hestrin, S. & Nicoll, R. A. (1989) *Science* **246**, 815–818.
13. Friedman, A. & Gutnick, M. J. (1989) *Eur. J. Neurosci.* **1**, 374–381.
14. Fox, A. P., Nowycky, M. C. & Tsien, R. W. (1987) *J. Physiol. (London)* **394**, 149–172.
15. Tang, C.-M., Presser, F. & Morad, M. (1988) *Science* **240**, 213–215.
16. Mayer, M. L., MacDermott, A. B., Westbrook, G. L., Smith, S. J. & Barker, J. L. (1987) *J. Neurosci.* **7**, 3230–3244.
17. Segal, M. & Manor, D. (1992) *J. Physiol. (London)* **448**, 655–676.
18. Alford, S., Frenguelli, B. G., Schofield, J. G. & Collingridge, G. L. (1993) *J. Physiol. (London)* **469**, 693–716.
19. Perkel, D. J., Petrozzino, J. J., Nicoll, R. A. & Connor, J. A. (1993) *Neuron* **11**, 817–823.
20. Nicoll, A., Larkman, A. & Blakemore, C. (1993) *J. Physiol. (London)* **468**, 693–710.
21. Henzi, V. & MacDermott, A. B. (1992) *Neuroscience* **46**, 251–273.
22. Rasmussen, H. & Barrett, P. Q. (1984) *Physiol. Rev.* **64**, 938–983.
23. Guthrie, P. B., Segal, M. & Kater, S. B. (1991) *Nature (London)* **354**, 76–79.
24. Müller, W. & Connor, J. A. (1991) *Nature (London)* **354**, 73–76.
25. Deisz, R. A., Fortin, G. & Zieglgänsberger, W. (1991) *J. Neurophys.* **65**, 371–380.